ELSEVIER

Journal of Alloys and Compounds 464 (2008) 418–421

Journal of ALLOYS AND COMPOUNDS

www.elsevier.com/locate/jallcom

Ethanol-assisted synthesis of $Zn_{0.5}Fe_{2.5}O_4$ nanocrystals in thermal solvent of paraffin

Kong Xiangrong, Zang Jun, Yang Xiaowei, Zeng Yanwei *

School of Materials Science and Technology, Nanjing University of Technology, No. 5 New Model Road, Nanjing 210009, PR China

Received 15 April 2007; received in revised form 1 October 2007; accepted 2 October 2007
Available online 7 October 2007

Abstract

In the atmosphere of N_2, low cost paraffin slices were refined and then successfully utilized as a solvent instead of the expensive high-carbon alkanes or alkenes like 1-octadecene to synthesize $Zn_{0.5}Fe_{2.5}O_4$ nanocrystals at 320 °C. In the experiments, the precursor solutions of ferric and zinc oleates were stoichiometrically prepared and injected by two-step operations into the hot solvent, together with controlled amounts of ethanol to tailor their thermal decomposition performances. The synthesized $Zn_{0.5}Fe_{2.5}O_4$ nanocrystals were characterized by XRD and FESEM, having uniform morphology and a quasi-monodisperse size distribution with a mean value 25 nm and a standard deviation of ±12.3%. The formation and structural characteristics of $Zn_{0.5}Fe_{2.5}O_4$ nanocrystals are attributed to the catalysing function of ethanol and the effective separation of nucleation and growth of nanocrystals via the two-step injections of reactive precursors.

Keywords: $Zn_{0.5}Fe_{2.5}O_4$ nanocrystals synthesis; Solvo-thermal process; Ethanol-assisted decomposition

1. Introduction

The oxide nanocrystals with plentiful physical properties continue to be of immense interest and importance for future high-tech applications. Among their significant characteristics are controlled manipulation and assembly of nanocrystals, which allow for the possible incorporation of nanoparticles into miniaturized electronic or photoelectronic devices [1,2]. In addition to its useful ferromagnetism as a traditional magnetic material, $Zn_{0.5}Fe_{2.5}O_4$ is also of great importance as high-quality magneto-resistance materials due to its high spin polarization and the tunnelling magneto-resistance effect at grain-boundaries [3–6]. In recent years, many transition metal oxides such as iron oxide, manganesian ferrite, cobalt ferrite, nickel ferrite have been successfully synthesized with solvo-thermal method [7–10], which are advantageous over other methods in the exquisite control over the chemical composition, size and shape of nanocrystals [11–14]. Unfortunately, however, there has been no report on the preparation of $Zn_{0.5}Fe_{2.5}O_4$ nanocrystals via solvo-thermal process. It is partially because ferric and zinc oleates start to decompose at different temperatures (much higher for the latter than the former), and the boiling points of commonly available solvents such as 1-hexadecylene, 1-octadecylene, octaether are not high enough to ensure the decomposition of ferric and zinc oleates. In this paper, we report on the preparation of $Zn_{0.5}Fe_{2.5}O_4$ nanocrystals by utilizing the refined paraffin, with a boiling temperature of 365 °C, as a thermal solvent in N_2 atmosphere to prevent it from oxidation. Moreover, an appropriate amount of ethanol was introduced into the hot solvent to tailor the decomposition thermodynamics and kinetics of ferric and zinc oleates and, then, to promote the synergetic reaction between the relevant chemical species to form $Zn_{0.5}Fe_{2.5}O_4$ nanocrystals.

2. Experimental

2.1. Synthesis of $Zn_{0.5}Fe_{2.5}O_4$ nanocrystals

Before the thermo-solvent synthesis, the raw paraffin was subjected to a refine treatment with a lab-setting, as schematically shown in Fig. 1. The paraffin slices were put into a three-necked flask, heated to 250 °C, 300 °C and 350 °C, respectively, and refluxed for 2 h at each point in N_2 atmosphere. With the nitrogen flowing out, the low-boiling point components were removed from the paraffin liquid and collected on the coiled condenser tube. After refining, the paraffin was measured to have a boiling temperature of 365 °C.

* Corresponding author. Tel.: +86 25 83587254; fax: +86 25 83587254.
E-mail address: zengyanwei@tom.com (Z. Yanwei).

0925-8388/$ – see front matter © 2007 Elsevier B.V. All rights reserved.
doi:10.1016/j.jallcom.2007.10.007

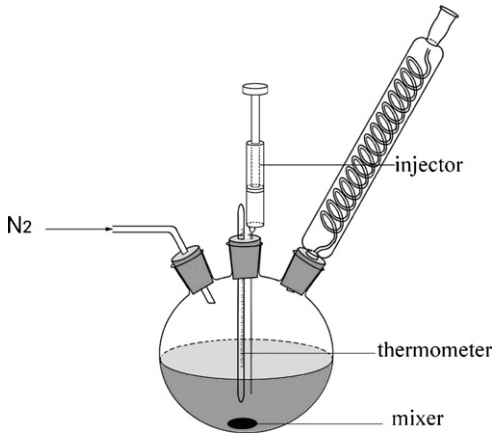

Fig. 1. Lab-setting for thermo-solvent synthesis.

As the precursors for synthesis of $Zn_{0.5}Fe_{2.5}O_4$ nanocrystals, the ferric and zinc oleates were obtained by reacting iron and zinc chlorides ($FeCl_3{\cdot}6H_2O$, $ZnCl_2$) with sodium oleate. In a practical synthetic operation, 0.136 g of zinc chloride ($ZnCl_2$, 1 mmol) and 0.609 g of sodium oleate (2 mmol) were introduced into a solvent mixture composed of 20 ml ethanol, 15 ml deionized water and 35 ml hexane. It was then heated to 70 °C under stirring and maintained at that temperature for 4 h. When the reaction was completed, the upper organic layer containing zinc oleate was separated from the lower aqueous phase and rinsed with deionized water to remove the surface pollutant ions. The pure zinc oleate was finally obtained by evaporating hexane away at 60 °C for 8 h. In the same way, the iron oleate was obtained by reacting 2.189 g ferric chloride ($FeCl_3{\cdot}6H_2O$, 5 mmol) with 4.568 g sodium oleate (15 mmol).

The procedure to synthesize $Zn_{0.5}Fe_{2.5}O_4$ nanocrystals is schematically illustrated in Fig. 2. For each batch, a precursor solution with 4.752 g ferric oleate (5 mmol), 0.653 g zinc oleate (1 mmol) and 0.2 ml oleic acid dissolved in 20 ml petroleum ether was used, in which a controlled volume of ethanol was added so as to promote the synergetic decompositions of these two oleates.

In order to obtain monodispersed nanocrystals, two-step injection operation was adopted according to the basic principles of "size distribution focusing technique" [11]. At the beginning of synthetic reaction, 1 ml of the precursor solution was first injected at one time into the hot liquid paraffin (heated in a three-necked flask at 320 °C) to boost the nucleation of $Zn_{0.5}Fe_{2.5}O_4$. After a short time interval, the rest of precursor solution was introduced in drops with an average speed of 0.1 ml/min to control the growth of $Zn_{0.5}Fe_{2.5}O_4$ nanocrystals. To study the influence of ethanol on the formation of $Zn_{0.5}Fe_{2.5}O_4$ nanocrystals, three schemes for ethanol incorporation were arranged: (1) no ethanol at all; (2) 5 ml ethanol; (3) 15 ml ethanol for each batch.

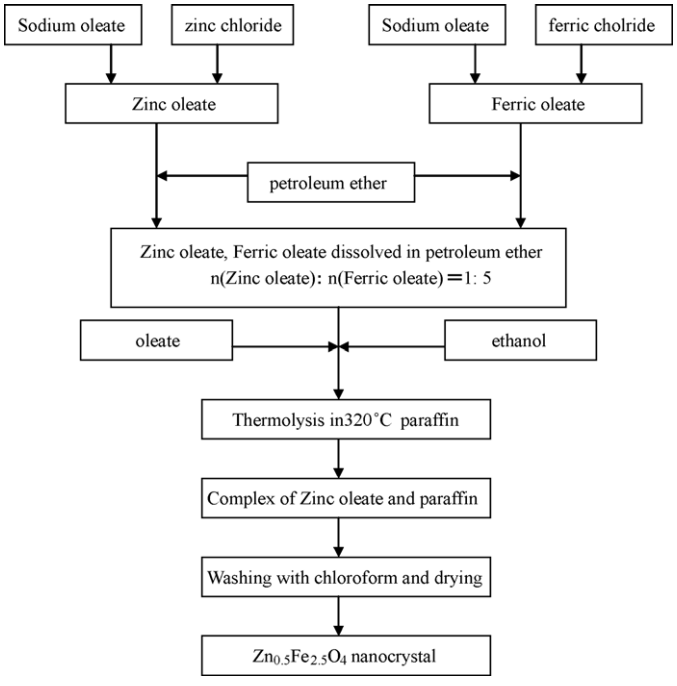

Fig. 2. The experimental flow-chart for $Zn_{0.5}Fe_{2.5}O_4$ nanocrystal by thermo-solvent method.

When the reaction was completed, the reaction system was cooled to the room temperature with the $Zn_{0.5}Fe_{2.5}O_4$ nanocrystals being dispersed in solid paraffin. In order to separate the nanocrystals from paraffin, chloroform was used to dissolve and then remove the paraffin with the help of ceramic separation membranes. In the end, the nanocrystals were washed with ethanol for 3 times and dried at 60 °C for 24 h.

2.2. Characterization of $Zn_{0.5}Fe_{2.5}O_4$ nanocrystals

For the phase identification of synthetic powder products, XRD analysis was carried out for all the samples with the diffractometer (Cu Kα, Rigaku, Japan) operating at 40/40 kV/mA and the 2θ ranging from 20° to 80°. In order to correctly differentiate $Zn_{0.5}Fe_{2.5}O_4$ and Fe_3O_4 by XRD due to their very similar crystal structures of cubic spinel-type, the freshly synthesized powders were fired at 600 °C before XRD analysis. This is because the Fe_3O_4 phase can be easily transformed into α-Fe_2O_3 with hexagonal structure when heated to 400 °C in air, while no transformations may happen with $Zn_{0.5}Fe_{2.5}O_4$. The morphology of the synthesized nanocrystals was observed using LEO-1530VP field-emission scanning electron microscopy (FESEM).

3. Results and discussion

3.1. The evaluation of paraffin as a thermal solvent

For the synthesis of oxide nanocrystals, the molecular polarization of solvents usually has a great influence on the nucleation and growth of nanocrystals [15]. It has been well understood that when a solvent has high molecular polarity, the crystal's growth in it may be affected and deviate from its own habit though sometimes such a deviation can be made use of for some special purposes. The paraffin molecules are mainly composed of alkyls with no polarity and, therefore, can provide a homogeneous and no-intervention environment for the crystal's growth. Moreover, the refined paraffin used in the present synthetic operation was observed to possess very stable chemical properties up to its boiling point 365 °C while it is protected in N_2 atmosphere. This greatly expands the availability of organic solvents with high boiling temperatures and low costs for wet chemical synthesis of oxide nanocrystals.

In addition, the hot paraffin liquid is a good solvent for a wide variety of organic precursors and the required synthetic reactions for nanocrystal growth may be taking place homogeneously in it. On the other hand, the paraffin itself can be easily dissolved in various organic solvents like chloroform, etc. This characteristic greatly facilitates the separation of synthesized nanocrystals from paraffin.

3.2. $Zn_{0.5}Fe_{2.5}O_4$ nanocrystals formation catalysed by ethanol

The synthetic products obtained by above-mentioned three schemes were first checked by XRD for phase identification before calcination at 600 °C. It was found that all the samples dis-

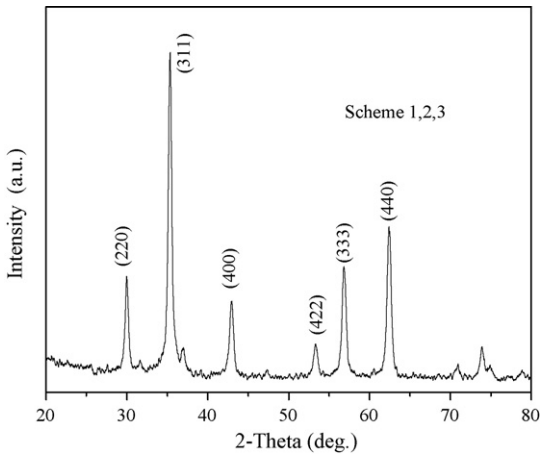

Fig. 3. The typical XRD diagram of synthetic products from solvo-thermal process of paraffin before calcination at 600 °C.

play the same XRD diagrams regardless of the different amounts of ethanol added in their solvo-thermal processes. The typical XRD diagram, as shown in Fig. 3, may be attributed to the spinel phase in comparison with PDF cards. Obviously, this result gives no full evidence to the formation of $Zn_{0.5}Fe_{2.5}O_4$ phase. Fig. 4 shows two XRD diagrams for the synthetic products after calcination at 600 °C. It is very interesting to note that the spinel phases in the samples obtained by Schemes 1 and 2 were turned into rhombohedral α-Fe_2O_3, as shown in the upper part in Fig. 4, while the samples with Scheme 3 retained their spinel structure, as shown in the lower part in Fig. 4. Consequently, it can be conclude that the spinel phase in the samples by Scheme 3 should be identified as $Zn_{0.5}Fe_{2.5}O_4$ and it can be obtained under the conditions of Scheme 3.

As to the influence of ethanol on the synthesis of $Zn_{0.5}Fe_{2.5}O_4$, it is believed that in the absence of ethanol, the zinc oleate may not decompose as quickly as ferric oleate does at 320 °C [9,10], and numerous Fe–O species in the heated solvent from the decomposition of ferric oleate are supposed to find overwhelming probability to form Fe_3O_4 phase due to the scarcity of Zn–O species. With the addition of ethanol, the esterification reaction between ethanol and oleates will take place and it may lower the energy barrier for the thermolysis of both oleates and promote the production of both Fe–O and Zn–O species in the solvent and, consequently, enhance the formation of zinc ferrite phase.

For a further understanding of the details of the synthetic reaction, however, we believe that the realistic synthesis of $Zn_{0.5}Fe_{2.5}O_4$ is closely associated with two kinetic parameters: the decomposing rates of ferric and zinc oleates and the stoichiometric collision probability of decomposition debris: Zn–O and Fe–O species in the liquid phase. When a small amount of ethanol is introduced into the reaction system, the actual catalysis of ethanol is rather low due to its remarkable evaporation. As a result, the zinc oleate decomposition is so slow that the stoichiometric collision of Zn–O and Fe–O species fails to happen, leading to no formation of $Zn_{0.5}Fe_{2.5}O_4$ nuclei. When an enough amount of ethanol is used as in Scheme 3, however, the decomposition of zinc oleate can be effectively catalysed and the concentration of Zn–O species may be greatly increased, resulting in a much higher probability of the stoichiometric collision between Zn–O and Fe–O species. Undoubtedly, the nucleation and crystal growth of $Zn_{0.5}Fe_{2.5}O_4$ will be remarkably boosted since the formation of $Zn_{0.5}Fe_{2.5}O_4$ thermodynamically has more favorable energy reduction than the concurrent formation of Fe_3O_4 and ZnO [16–19].

Fig. 5 is a typical FESEM micrograph of as-prepared $Zn_{0.5}Fe_{2.5}O_4$ nanocrystals from ethanol-assisted thermal solvent process of paraffin. It can be seen that the particles are quite uniform either in size or in morphology. According to the image analysis by simPCI software, the synthetic $Zn_{0.5}Fe_{2.5}O_4$ nanocrystals are evaluated to have an average grain size of 24.79 nm with a standard deviation of ±12.3%.

It is believed that such a quasi-monodispersion of grain sizes is mainly the result of our two-step injections of precursor solution. It can effectively separate the nucleation and the growth of $Zn_{0.5}Fe_{2.5}O_4$ nanocrystals. The first injection of limited precursors is supposed to satisfy the formation of $Zn_{0.5}Fe_{2.5}O_4$

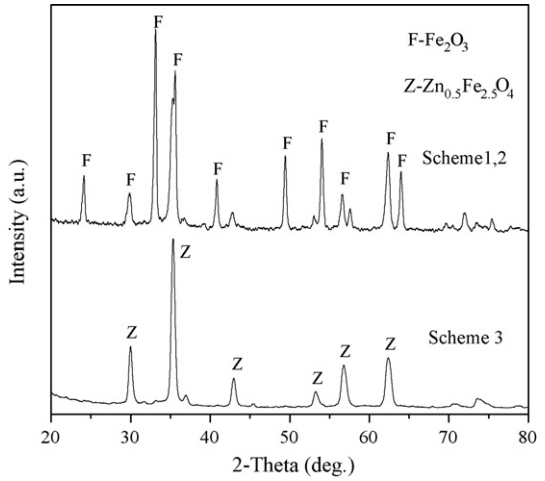

Fig. 4. Two XRD diagrams of the synthetic products from solvo-thermal process of paraffin after calcination at 600 °C.

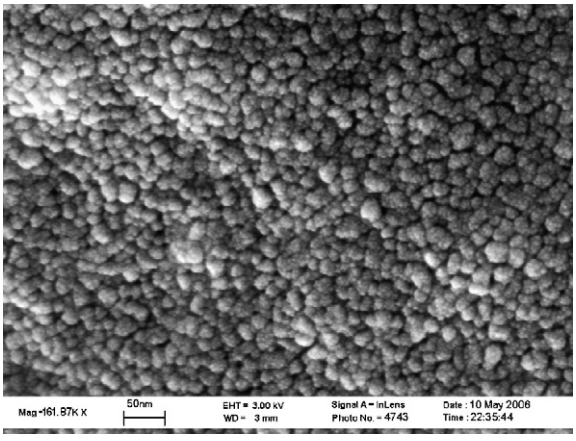

Fig. 5. FESEM image of $Zn_{0.5}Fe_{2.5}O_4$ nanocrystals from ethanol-assisted thermal solvo-thermal process of paraffin.

nuclei, whereas the following additions of the precursors under close control practically feed the materials for the growth of each $Zn_{0.5}Fe_{2.5}O_4$ nucleus in terms of the size-distribution focusing principles [11]. In addition, another important factor that favors the narrow size distribution should be the effective inhibition of possible Ostwald ripening process when the M–O (M=Zn or Fe) species are reduced and depleted in the later stage of synthesis. This is because no free oleate ligands are present in the solution due to the esterification reaction between ethanol and oleates, which are necessary for stabilizing the M–O species [10], and, therefore, makes contribution to the stability of quasi-monodispersed $Zn_{0.5}Fe_{2.5}O_4$ nanocrystals.

4. Conclusion

(1) For the first time, the refined paraffin was successfully utilized as a solvent in solvo-thermal process to prepare oxide nanocrystals by using N_2 gas as protective atmosphere. Compared to the usually used high-carbon alkanes or alkenes like 1-octadecene, the refined paraffin is a good solvent for the syntheses of oxide nanocrystals because of its good chemical stability, high boiling temperature, easy separation, easy availability and low prize, etc.
(2) Ethanol was successfully used as a catalyst to tailor the decomposition kinetics of zinc and ferric oleates through the irreversible esterification reactions, which are found to greatly promote the decomposition reactions and, therefore, enhance the stoichiometric collision between Zn–O and Fe–O species for the formation of $Zn_{0.5}Fe_{2.5}O_4$.
(3) The as-prepared $Zn_{0.5}Fe_{2.5}O_4$ nanocrystals are characterized by uniform morphology and quasi-monodispersion in size, having an average size of 25 nm and a standard deviation of ±12.3%. These microstructural features are mainly attributed to the effective separation of nucleation and growth of nanocrystals via the two-step injections of reactive precursors.

Acknowledgment

The authors would like to gratefully acknowledge the financial support from The Science Foundation of Jiangsu, PR China (Grant BK2006182, 06KJA43008).

References

[1] Y. Bao, M. Beerman, A.B. Pakhomov, K.M. Krishnan, J. Phys. Chem. B 109 (2005) 7220.
[2] G. Li, L. Li, J. Boerio-Goates, B.F. Woodfield, J. Am. Chem. Soc. 127 (2005) 8659.
[3] S. Yan, J. Geng, Y. Li, E. Zhou, J. Mag. Mag. Mater. 277 (2004) 84.
[4] G. Hua, Y. Liu, J. Chen, Chem. Res. 14 (2003) 9.
[5] N. Nishimura, T. Hirai, A. Koganei, T. Ikeda, K. Okano, Y. Sekiguchi, Y. Osada, J. Appl. Phys. 91 (2002) 5246.
[6] W. Kula, J. Wolfman, K. Ounadjela, E. Chen, W. Koutny, J. Appl. Phys. 93 (2003) 8373.
[7] N.R. Jana, Y. Chen, X. Peng, Chem. Mater. 16 (2004) 3931.
[8] M. Yin, S. O'Brien, J. Am. Chem. Soc. 125 (2003) 10180.
[9] J. Park, K. An, Y. Hwang, J. Park, H. Noh, J. Kim, J. Park, N. Hwang, T. Hyeon, Nat. Mater. 12 (2004) 891.
[10] Y. Chen, M. Kim, G. Lian, M.B. Johnson, X. Peng, J. Am. Chem. Soc. 127 (2005) 13331.
[11] Y. Yin, A.P. Alivisatos, Nature 437 (2005) 664.
[12] B.L. Cushing, V.L. Kolesnichenko, C. O'Connor, J. Chem. Rev. 104 (2004) 3893.
[13] M.P. Pileni, Nat. Mater. 2 (2003) 145.
[14] P.A. Bianconi, J. Lin, A.R. Strzelecki, Nature 349 (1991) 315.
[15] C. Burda, X. Chen, R. Narayanan, M.A. El-Sayed, Chem. Rev. 105 (2005) 1025.
[16] S. Qu, H. Yang, D. Ren, S. Kan, G. Zou, D. Li, M. Li, J Colloid Interface Sci. 215 (1999) 190.
[17] A. Kundu, S. Anand, H.C. Verma, Powder Technol. 132 (2003) 131.
[18] W. Kim, F. Saito, Powder Technol. 114 (2001) 12.
[19] X. Shi, C. Li, D. Wang, Chem. World 43 (2002) 451.